

Source localization techniques with acoustic arrays

H.M.M. van der Wal, P. Sijtsma

National Aerospace Laboratory NLR, The Netherlands, Email: vdwal@nlr.nl, sijtsma@nlr.nl

Introduction

Acoustic antennas are widely used for source localization, both close to and away from the source. NAH (Nearfield Acoustic Holography) is an experimental method for source localization and quantification, measuring in the acoustic nearfield of the source. On the other hand, the beamforming technique is suited for the farfield. This paper will address both methods. At NLR and DNW, beamforming is applied on routine basis on stationary and rotating sources in wind tunnels. Outdoors, moving sources have been measured as well, both translating (aircraft flying over) and rotating sources (wind turbines). For these sources, appropriate adaptations on the beamforming algorithm were made. In addition, techniques were developed to increase the accuracy of the source strength of the partial sound sources, determined from array measurements. A new development is in-duct beamforming, localizing and quantifying sources on the rotor and stator of an aero engine.

Nearfield acoustic holography

NAH (Nearfield Acoustic Holography) is an experimental method for reconstruction of the complete sound field close to a test object (sound source or sound radiating surface) from sound pressure measurements on many positions, located on a surface enclosing the test object, in its acoustic nearfield. A detailed description can be found in reference [1]. This technique has been applied on the sound, radiated from a composite fuselage barrel, which was excited with a sound source inside. The sound pressures were measured with a phased array of 64 microphones, traversing in axial directions (64 positions). The normal velocity at the barrel surface was determined from the measured sound pressure data using spatial Fourier transforms, for details see reference [2]. Figure 1 shows the set-up and a typical result for the 800 Hz 1/3 octave band, in terms of a map of the normal velocity of the barrel surface. Red spots in this plot have a relatively high surface velocity, which is consistent with a relatively low sound insulation.

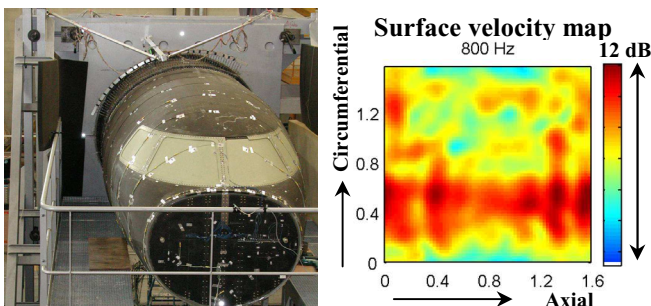


Figure 1: Composite fuselage barrel with traversing phased array for nearfield acoustic holography measurements, including typical results (normal barrel surface velocity).

Beamforming techniques

Conventional beamforming

A description of beamforming techniques can be found in text books [3] or on internet. In order to provide an intuitive understanding of the technique, the “delay and sum” technique in the time domain is outlined. The principle of this method is summation of the array microphone signals with varying delays. These delays correspond with different path lengths (and corresponding transmission times) between a supposed point source on a given position (“scan point”), with a source strength yet unknown, and the various array microphones. This summation is successively done for a number of “scan points” in a “scan plane”, where the real sound sources are assumed to be located. The time delays correspond with phase differences, which depend also on the frequency. For a scan point coinciding with a sound source, the delayed signals add up to a significant value, proportional to the strength of the corresponding sound source. For a scan point not coinciding with a sound source, the delayed signals add up to a small residue. In this way, by constructive and destructive interference, the source strength distribution over the scan points can be determined. A plot of the source strength distribution in the scan plane is called a “source map”. If the distance between the array and the sound sources (i.e. the scan plane) is large, compared to the array dimensions, “conventional beamforming” is identical to “delay and sum”.

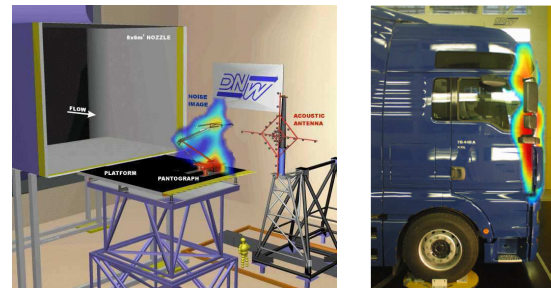


Figure 2: Left: high-speed train pantograph & “spider web” array. Right: full-scale MAN-truck, both in DNW-LLF.

Wind tunnel applications

Early array applications at NLR/DNW were developed for noise source localization on wind tunnel models, first for anechoic wind tunnel models (e.g. pantograph, Figure 2). The next development was to apply phased arrays in closed wind tunnels. Examples are a truck (Figure 2), and a Fokker 100 half model without and with flap tip fence (Figure 3). For array testing in closed wind tunnels, a wall mounted array is commonly used, having typically 100 microphones, as shown in Figure 3. If directivity information is required, multiple arrays can be mounted on the wall, floor or ceiling of the wind tunnel test section. See reference [4] for more detailed information about array testing in NLR/DNW wind tunnels.

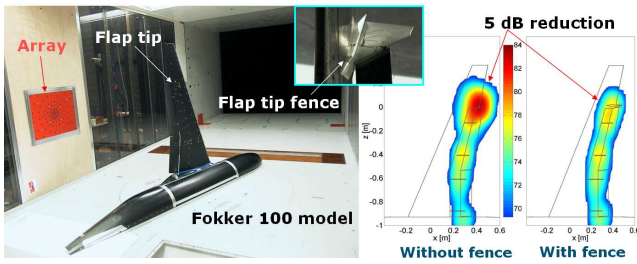


Figure 3: Flap noise measurement in DNW-LST wind tunnel. Right: noise source maps without and with flap tip fence, showing a noise reduction of 5 dB.

Moving sources

A further step in NLR array technology is quantitative noise source classification on moving sources, in particular on aircraft flying over, although applicable on ground vehicles as well. Figure 4 shows the set-up, used at Schiphol, close to the Kaagbaan runway. The two lateral arrays in Figure 4 were used in order to determine directivity effects. For aircraft flying over, the scan plane has to move as well, along with the aircraft, so that the noise source positions relative to the scan plane remain unchanged during the data acquisition (“moving focus”). For this, the aircraft position during data acquisition should be measured, synchronic with the microphone data.

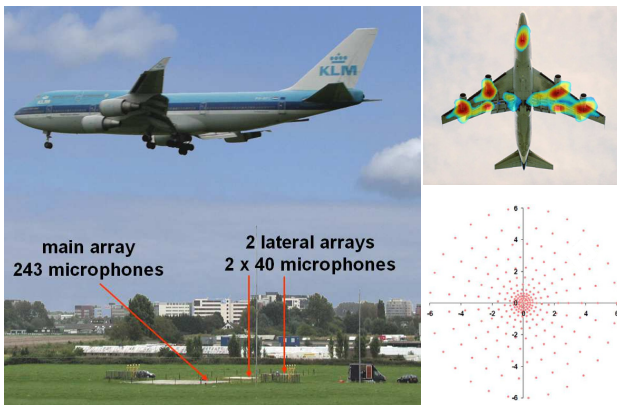


Figure 4: Flyover measurements at Schiphol Airport. Left: array set-up. Lower right: Main array design. Upper right: typical noise source map for a B747.

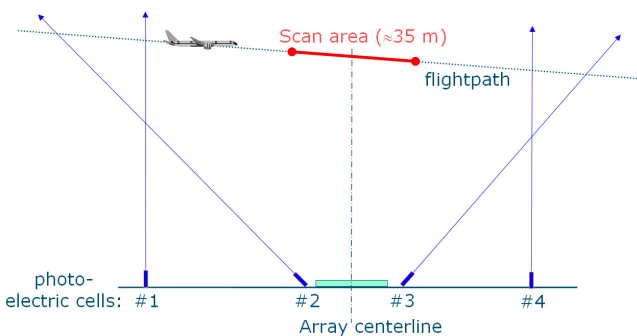


Figure 5: Flyover measurements at Schiphol Airport, set-up for aircraft position measurement.

A method to achieve this is depicted in Figure 5. Four photo-electric cells and the array microphones are connected to the same data acquisition system. The time signals of 4 photo cells are cross correlated to determine the time differences on passing of the blue lines (in Figure 5) by the aeroplane. From the signals of the cells #1 and #4 and the distance

between these cells, the flight speed (assumed constant) can be calculated. The aircraft altitude at cell #1 is calculated from the signals of the cells #1 and #2, the distance between these cells and the elevation angle of cell #2. The same procedure is performed for cells #3 and #4. For further details of the array technique applied by NLR for moving sources, see references [5], [6] and [7].

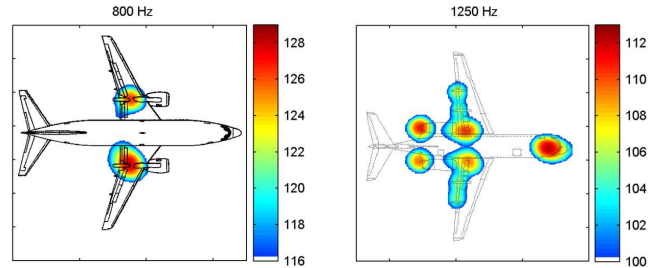


Figure 6: Typical noise source maps of a noisy aircraft (left, engines dominate) and a quiet aircraft (right, also airframe sources contribute).

Figure 6 shows typical source maps of both a noisy and a quiet aircraft. Besides the (16 dB) lower maximum level on the dB-scale next to the source maps, also airframe noise sources (flaps and landing gear) contribute to the source map on the right, where the noise radiation in the left plot is dominated by the (noisy) engines.

Rotating sources

For rotating sources, such as wind turbine rotors, post processing with a non moving scan plane is possible (“stationary focus”). The left picture of Figure 7 shows a typical result: the noise sources are spread out over the scan plane. If the scan plane rotates along with the rotor (“rotating focus”), the sound source positions are visible more accurately. For this type of post processing, the position of the rotor blades should be determined. Usually, the rotor blade positions are determined from a “1/rev” pulse, which is generated each time that one of the blades is on a specific position. See reference [8] for further details.



Figure 7: Wind turbine field test, post processing with stationary focus (left) and rotating focus (right).

In Figure 7, the (downwards moving) blade at the right side seems to radiate more noise than the two blades on the left. This is due to the directivity of the radiated sound of a rotor blade: in forward direction the blade radiates more noise than in backward direction. So, in the direction of the array, located on the ground, a downward moving blade emits more noise than a blade moving in upward direction.

Source integration techniques

For both data reduction and more accurate source levels, a source integration technique is used, described as the “simplified method” in reference [9], also discussed in reference [4]. Herein, a number of areas of interest (integration areas) on the scan plane are allocated (rectangles in Figure 8, upper right). On these areas, the source powers obtained by beamforming of all scan points are summed. The result is then divided by the summation of all source powers obtained with a simulated monopole point source (point spread function) in the centre of the integration area. Finally, this ratio is multiplied with the acoustic source power of this point source. The ACF (Array Calibration Function) is defined as the ratio of the sum of the source powers over all scan points after correction and the same sum before correction. The thus obtained integrated source powers give a fairly good estimate of the actual source power radiated from that area. See also references [7] and [10] for more information on source integration.

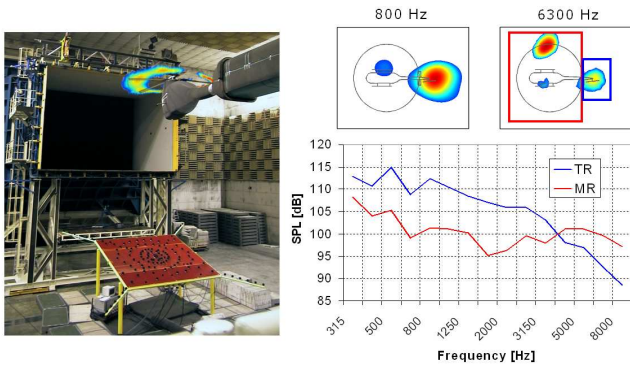


Figure 8: Helicopter test in DNW-LLF, including source spectra of tail and main rotor, determined with source integration over the surfaces, indicated by the red and blue rectangles.

Figure 8 shows an example of the source integration for the sources on the main and tail rotor of a helicopter model. The integration contours are indicated by the red and blue rectangles in upper right source map in Figure 8. The 1/3 octave band spectrum of the strengths of both sources, calculated by source integration, is also given in this figure.

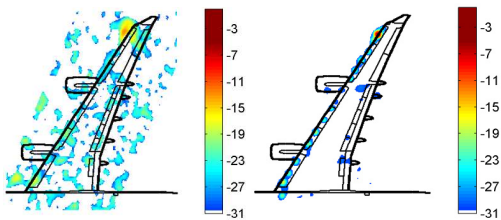


Figure 9: Airbus A340 1:10.6 scale model in the DNW-LLF closed test section. Source plots at 12360 Hz, Conventional Beamforming (left) and CLEAN-SC (right).

A new deconvolution method improving the resolution of beamforming results is “CLEAN-SC”, see reference [11]. The merits were demonstrated using airframe noise measurements on a scale model of the Airbus A340. It was found that CLEAN-SC is a very effective tool to remove dominant sources from source plots, thereby unmasking secondary sources. Like other deconvolution algorithms,

significant improvements in spatial resolution were found. Moreover, CLEAN-SC is able to extract absolute values of source components from the source plots. Summed results of these source powers agree very well with results of the conventional source integration method discussed above.

In-duct beamforming

Beamforming techniques have also been applied to fan rig measurements with a circular microphone array in the engine intake duct wall, see Figure 10, which is normally used for circumferential mode detection (described in reference [12], not discussed here). Both stationary and rotating focus processing are useful. The contributions of tonal noise (buzz-saw noise, rotor alone noise, fan-stator interaction) and broadband engine noise (fan-broadband noise) are considered separately.

At lower engine speeds, typically during approach, fan-broadband noise is a major component of the total noise emitted from turbofan engines, as is illustrated by Figure 11. This broadband noise can be caused by various possible mechanisms: interaction of the intake duct boundary layer with the rotor blade tips, interaction of the turbulent rotor wakes with the stator vanes, rotor blade self noise (trailing edge noise), and stator vane self noise.

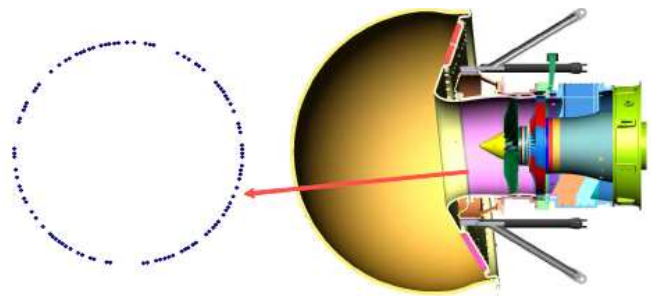


Figure 10: Drawing of fan rig, provided by Assystem UK Ltd; the mode detection array is located on the grey strip in the intake.

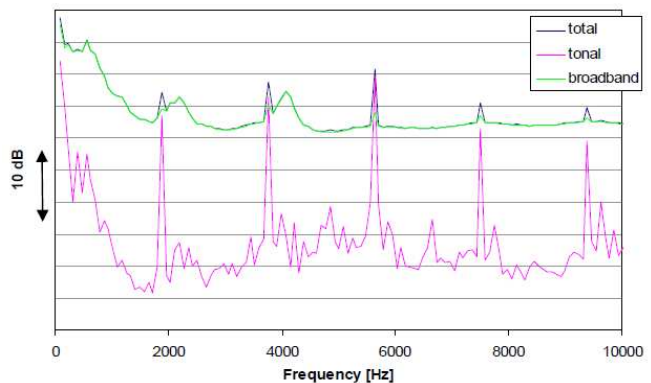


Figure 11: Average auto-spectrum at microphone array in Figure 10, + breakdown into tonal and broadband noise.

Using mode detection and phased array techniques, we are able to explore many properties of the source mechanisms causing the spectral humps in the broadband noise, see Figure 11, like:

- their broadband (non rotor-bound) nature,
- their modal content,
- frequencies of unsteady loading at the rotor,
- possible source locations on rotor and stator,

- their coherent behaviour.

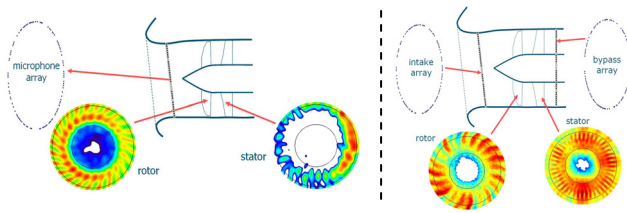


Figure 12: Beamforming results on rotor and stator with mode detection arrays in the intake (left) and both in the intake and bypass duct (right).

Figure 12 shows some in-duct beamforming results, obtained with arrays of 100 microphones in both the inlet and the bypass duct. Noise source locations on both rotor and stator are clearly visible. The noise sources on the stator vanes seem to be distributed along the span. Hence, tip noise sources seem to be of lower importance.

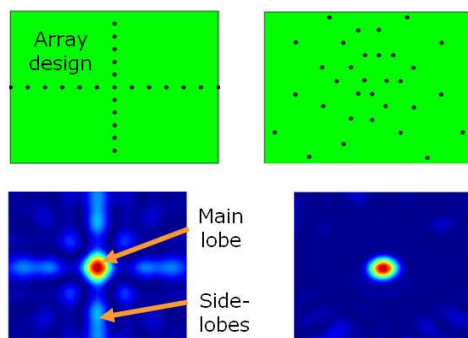
The bypass mode detection results seem to indicate that the noise sources are located at the trailing edges of the stator vanes. The mode detection results seem to indicate further that most noise in the intake is generated at the stator. The current status of in-duct mode detection and beamforming capabilities, available at NLR (see references [13] and [14]), is:

- Source localization by phased array beamforming techniques, both with stationary and rotating focus, applied on data measured with circular intake and bypass duct microphone arrays, is feasible.
- The breakdown into tonal and broadband noise gives valuable additional information.
- Knowledge about the (circumferential) modal content is very important to understand the beamforming results.

Array design

The array design for the beamforming techniques, discussed above, is such that the side lobes in the source maps are minimised, as is illustrated by Figure 13. For each specific application, the array design can be optimized.

Figure 13: Effect of the array design on the side lobes, both for a cross-shaped array and a sparse array.



Conclusions

Concerning the source localization methods discussed above, the following concluding remarks can be made.

- Array techniques are a powerful source localization tool, depending on the specific source configuration.
- Accurate quantification of source powers, determined with beamforming, is possible with source integration and array calibration functions.

- Combining different array techniques in aero engine ducts may provide additional information of noise sources.
- Many array techniques are available at NLR.

Acknowledgments

The research for this paper was performed in many projects. The public and private sponsors for these projects are acknowledged.

References

- [1] E. Williams. Fourier Acoustics. Academic Press, London, 1999
- [2] H. van der Wal, P. Sijtsma, B. Berton and P. Hardy. A novel reciprocal sound transmission measuring method, applied on a composite fuselage. 26th ICAS conference, Anchorage, AK, also NLR-TP-2008-382
- [3] D. Johnson and D. Dudgeon. Array signal processing. Prentice Hall signal processing series, Englewood Cliffs, 1993
- [4] P. Sijtsma. Phased array beamforming in wind tunnels. VKI/EWA Lecture series on "Experimental Aeroacoustics", also NLR-TP-2006-732
- [5] P. Sijtsma. Beamforming on moving sources. VKI/EWA Lecture series on "Experimental Aeroacoustics", also NLR-TP-2006-733
- [6] P. Sijtsma and H. van der Wal. Identification of Noise Sources on Civil Aircraft in Approach using a Phased Array of Microphones. NATO-RTO SET Symposium at Leri, Italy, 2004, also NLR-TP-2004-166
- [7] S. Oerlemans and P. Sijtsma. Determination of absolute levels from phased array measurements using spatial coherence, AIAA 2002-2464, also NLR TP-2002-226
- [8] P. Sijtsma, S. Oerlemans and H. Holthusen. Location of rotating sources by phased array measurements, AIAA 2001-2167, also NLR-TP-2001-135
- [9] T. Brooks and W. Humphreys Jr. Effect of directional array size on the measurement of airframe noise components, AIAA 99-1958, 1999
- [10] P. Sijtsma and R. Stoker. Determination of absolute contributions of aircraft noise components using fly-over array measurements. AIAA 2004-2958, also NLR-TP-2004-167
- [11] P. Sijtsma. A new deconvolution Technique to Improve the Resolution of Acoustic Source Plots from Microphone Array Measurements. AIAA 2007-3436, also NLR TP-2007-345
- [12] E. Rademaker, P. Sijtsma, B. Tester. Mode detection with an optimised array in a model turbofan engine intake at varying shaft speeds, AIAA 2001-2181, also NLR TP-2002-132
- [13] P. Sijtsma. Using phased array beamforming to locate broadband noise sources inside a turbofan engine, AARC Engine Noise Phased Array Workshop, Cambridge, MA, 2006, also NLR-TP-2006-320
- [14] P. Sijtsma, Feasibility of in-duct beamforming, AIAA 2007-3696, also NLR-TP-2007-348